Received: 12 January 2021 | Revised: 24 April 2021 | Accepted: 26 April 2021

DOI: 10.1002/hbm.25468

RESEARCH ARTICLE

WILEY

Pre-supplementary motor network connectivity and clinical outcome of magnetic stimulation in obsessive–compulsive disorder

Gong-Jun Ji[1,2,3,4] | Wen Xie[5] | Tingting Yang[1,3,4] | Qianqian Wu[1,3,4] | Pengjiao Sui[1,3,4] | Tongjian Bai[1,3,4] | Lu Chen[1,3,4] | Lu Chen[1,3,4] | Xingui Chen[1,3,4] | Yi Dong[5] | Anzhen Wang[5] | Dandan Li[1,3,4] | Jinying Yang[6] | Bensheng Qiu[7] | Fengqiong Yu[1,3,4] | Lei Zhang[1,3,4] | Yudan Luo[1,3,4] | Kai Wang[1,2,3,4] | Chunyan Zhu[1,3,4]

[1]Department of Neurology, The First Affiliated Hospital of Anhui Medical University, The School of Mental Health and Psychological Sciences, Anhui Medical University, Hefei, China

[2]Institute of Artificial Intelligence, Hefei Comprehensive National Science Center, Hefei, China

[3]Anhui Province Key Laboratory of Cognition and Neuropsychiatric Disorders, Hefei, China

[4]Collaborative Innovation Center of Neuropsychiatric Disorders and Mental Health, Hefei, Anhui Province, China

[5]Department of Psychiatry, Anhui Mental Health Center, Hefei, China

[6]Laboratory Center for Information Science, University of Science and Technology of China, Hefei, China

[7]Hefei National Lab for Physical Sciences at the Microscale and the Centers for Biomedical Engineering, University of Science and Technology of China, Hefei, China

Correspondence
Chunyan Zhu and Kai Wang, Laboratory of Cognitive Neuropsychology, The School of Mental Health and Psychological Sciences, Anhui Medical University, No. 81 Meishan Road, Shushan District, Hefei 230032, China.
Email: ayswallow@126.com (C. Z.) and wangkai1964@126.com (K. W.)

Funding information
The National Natural Science Foundation of China: 81771456, 31970979, 81971689, 8180111185, 82001429, 31771222, and 31571149; The Major Program of the National Natural Science Foundation of China: 82090034; Youth Top-notch Talent Support Program of Anhui Medical University; Collaborative Innovation Center of Neuropsychiatric Disorders and Mental Health of Anhui Province; National Key R&D Plan of China, Grant/Award Number: 2016YFC1300604; National Basic Research Program of China, Grant/Award Number: 2015CB856405; Doctoral Foundation of

Abstract

A large proportion of patients with obsessive–compulsive disorder (OCD) respond unsatisfactorily to pharmacological and psychological treatments. An alternative novel treatment for these patients is repetitive transcranial magnetic stimulation (rTMS). This study aimed to investigate the underlying neural mechanism of rTMS treatment in OCD patients. A total of 37 patients with OCD were randomized to receive real or sham 1-Hz rTMS (14 days, 30 min/day) over the right pre-supplementary motor area (preSMA). Resting-state functional magnetic resonance imaging data were collected before and after rTMS treatment. The individualized target was defined by a personalized functional connectivity map of the subthalamic nucleus. After treatment, patients in the real group showed a better improvement in the Yale–Brown Obsessive Compulsive Scale than the sham group ($F_{1,35} = 6.0$, $p = .019$). To show the neural mechanism involved, we identified an "*ideal target connectivity*" before treatment. Leave-one-out cross-validation indicated that this connectivity pattern can significantly predict patients' symptom improvements ($r = .60$,

Gong-Jun Ji and Wen Xie contributed equally to this work.

Anhui Medical University, Grant/Award Number: XJ201532

$p = .009$). After real treatment, the average connectivity strength of the target network significantly decreased in the real but not in the sham group. This network-level change was cross-validated in three independent datasets. Altogether, these findings suggest that personalized magnetic stimulation on preSMA may alleviate obsessive–compulsive symptoms by decreasing the connectivity strength of the target network.

KEYWORDS
functional connectivity, obsessive–compulsive disorder, supplementary motor area, transcranial magnetic stimulation

1 | INTRODUCTION

Obsessive–compulsive disorder (OCD) is the fourth most common psychiatric disease with a lifetime prevalence of 0.8–3.0% (Heyman, Mataix-Cols, & Fineberg, 2006). However, about 30–60% of patients fail to respond to traditional pharmacological or psychological treatment (Koran, Hanna, Hollander, Nestadt, & Simpson, 2007; Soomro, Altman, Rajagopal, & Oakley-Browne, 2008; Van Ameringen, Patterson, & Simpson, 2014). As a result, these patients are significantly affected by uncontrollable symptoms, such as obsessive thinking and compulsive behavior (Ruscio, Stein, Chiu, & Kessler, 2010). Recently, many clinical trials have investigated the efficacy of repetitive transcranial magnetic stimulation (rTMS) in treating OCD. Although the findings were mixed, meta-analyses indicated that active rTMS was clinically and statistically superior to sham treatment (Rehn, Eslick, & Brakoulias, 2018). The U.S. Food and Drug Administration has approved the use of deep rTMS on medial prefrontal and anterior cingulate cortex as an adjunct for the treatment of adult patients suffering from OCD (Lefaucheur et al., 2020). Particularly, a multicenter study indicated that 38% patients reached full response after 6 weeks deep rTMS stimulation, although the majority of patients were nonresponders (Carmi et al., 2019). To further improve the therapeutic effect, the underlying mechanism associated with stimulation protocols needs to be elucidated.

The human brain is a complex network supported by functional interaction of neural populations. However, this functional connectome also allows pathological perturbations to spread in a networked manner (Shafiei et al., 2020; Yau et al., 2018; Zhou, Gennatas, Kramer, Miller, & Seeley, 2012). Similarly, although a local region is directly stimulated by rTMS, the aftereffects may spread through the intrinsically organized connectome associated with the stimulated site (Beynel, Powers, & Appelbaum, 2020). For example, stimulation over the prefrontal cortex induced more connectivity alterations than stimulation over the visual cortex (Castrillon et al., 2020), and targeting a hub region impacted cognition more than targeting a nonhub region (Lynch et al., 2019). Similar phenomena were also found in deep brain stimulation (DBS). The connectivity profile of the DBS site significantly predicted clinical outcomes (Horn et al., 2017). Thus, the selection of the rTMS target is one of the most important factors related to the aftereffects, and the intrinsic connectivity pattern of the stimulation target is critical for understanding the mechanism of action.

Many randomized and sham-controlled trials investigated the clinical efficacy of rTMS in OCD. However, most were small sample studies with varied parameters with regard to the stimulation target (e.g., dorsal prefrontal cortex and supplementary motor area [SMA]), frequency (e.g., 1 and 10 Hz), duration (1–6 weeks), and number of total pulses (7,500–60,000) (Rehn et al., 2018). A meta-analysis indicated that low-frequency rTMS over the SMA may offer the greatest effectiveness in OCD (Rehn et al., 2018). The anterior part of the SMA (preSMA) is a crucial node of response inhibition network (Johansen-Berg et al., 2004). Its connection with the subthalamic nucleus (STN) is important to suppress responses that are no longer required or inappropriate (Bari & Robbins, 2013; Hampshire & Sharp, 2015). A double-blind multicenter study indicated that DBS on the STN could significantly reduce the symptoms of OCD (Mallet et al., 2008). From a network perspective, Fox et al. suggested that the effective target for rTMS could be identified through resting-state functional connectivity (FC) of the DBS site (Fox et al., 2014). In clinical application, this personalized target may improve treatment efficacy, similar to the findings from major depression treatment (Fox, Buckner, White, Greicius, & Pascual-Leone, 2012; Weigand et al., 2017).

Using a double-blind, randomized, sham-control design, we initially tested the clinical efficacy of an rTMS protocol with personalized targets. Then, resting-sate functional MRI (fMRI) data were utilized to elucidate the underlying neural mechanism. We predicted that the target network plays an important role in mediating the treatment effect.

2 | METHODS

2.1 | Standard protocol approvals, registrations, and patient consents

The study protocol was reviewed and approved by the institutional ethics committee of Anhui Medical University (Hefei, China). All participants provided written, informed consent before the experiments according to the Declaration of Helsinki. Data of this study were part of a clinical trial registered at ClinicalTrials.gov (NCT03393078). Since this study focused on the network mechanism of rTMS treatment on obsessive–compulsive symptoms, the second outcomes of the trial were not included here.

2.2 | Study design

According to a previous study (Hawken et al., 2016), a parallel two-arm model (1:1; mean difference = 9.5 and *SD* = 9.1), yielded a sample size of 15 patients for each arm, providing 80% power with α level = .05. Participants were randomly separated into two groups by random number generation, and received real or sham rTMS over the right preSMA for 14 consecutive days (experiment Days 1–14). A researcher who was not involved in any aspect of the trial performed the random separation of participants. Structural, fMRI and symptom data were acquired for each participant on the first experiment day before treatment, and the next day after the end of treatment. Patients and raters were blinded to the group information. Except during clinical assessment, the raters did not take any other part in this study.

2.3 | Subjects

Thirty-seven participants were enrolled from the First Affiliated Hospital of Anhui Medical University and the Anhui Mental Health Center (Hefei, China). The inclusion criteria were as follows: (a) diagnosed by more than two clinical psychiatrists (Y. D., and W. X.), with DSM-5 diagnostic criteria for OCD; (b) the Hamilton Depression Rating Scale score was less than 17 points; (c) no significant improvement in symptoms after taking one or more types of anticompulsive medication, or no history of taking any anticompulsive medication; (d) a stable doses of medication has been taken for more than 4 weeks and could be kept during the following rTMS treatment; (e) aged between 18 and 50 years old; and (f) both the patient and family agreed to participate in this study.

Exclusion criteria were: (a) patients with unstable physical conditions, pregnancy and breastfeeding; (b) nonmovable metal objects around the head or inside the head; (c) increased intracranial pressure due to infarcts or trauma; (d) a history of addiction, neurological diseases, or head injury; (e) concurrent comorbidities with other psychiatric disorders; and (f) previously received rTMS treatment.

2.4 | MRI data acquisition and preprocessing

Anatomic and resting-state functional MRI data were acquired with a 3-T scanner (Discovery 750; GE Healthcare, Milwaukee, WI) (Ji et al., 2018). High spatial resolution T1-weighted anatomic images were acquired in the sagittal orientation using a three-dimensional brain-volume sequence (repetition/echo time, 8.16/3.18 ms; flip angle, 12°; field of view, $256 \times 256\ mm^2$ 256×256 matrix; section thickness, 1 mm, without intersection gap; voxel size, $1 \times 1 \times 1\ mm^3$ 188 sections). Functional MRI data were acquired in the resting state. Participants were instructed to rest with their eyes closed without falling asleep. Functional images (217 volumes) were acquired using a single shot gradient-recalled echo planar imaging sequence (repetition/echo time, 2,400/30 ms; flip angle, 90°). Images of 46 transverse sections (field of view, $192 \times 192\ mm^2$ 64×64 in-plane matrix; section thickness without intersection gap, 3 mm; voxel size, $3 \times 3 \times 3\ mm^3$) were acquired parallel to the anteroposterior commissure line.

Functional images were processed using SPM12 (www.fil.ion.ucl.ac.uk/spm). Briefly, the preprocessing included the following steps: (a) deletion of the first five volumes; (b) slice timing and realignment; (c) co-registration of structural to functional images; (d) normalization of functional images by DARTEL-based structural segmentation; (e) smoothing of functional images with a 4-mm isotropic Gaussian kernel; (f) temporal band-pass filtering (0.01–0.1 Hz); and (g) regressing out 27 nuisance signals (three averages from cerebrospinal fluid, global brain, and 24 head motion parameters (Friston, Williams, Howard, Frackowiak, & Turner, 1996)).

2.5 | Personalized rTMS treatment

TMS was performed using a Magstim Rapid^2 stimulator (Magstim Company, Whitland, UK) with a 70-mm air-cooled figure-of-eight coil. All stimulations were guided by the participant's anatomical image and a frameless neuronavigation system (Brainsight; Rogue Research, Montreal, Canada).

On each treatment day, patients received real or sham 1-Hz rTMS, which lasted 30 min. The active rTMS was applied to the preSMA with an intensity of 110% of the individual resting motor threshold (RMT). RMT was defined as the lowest intensity evoking a small response (>50 μV) in more than five of 10 consecutive trials. During treatment, the coil was maintained horizontally, with its center positioned over the preSMA to maximize the strength of the electric field perpendicular to the target area (Fox et al., 2004; Janssen, Oostendorp, & Stegeman, 2015). We chose the preSMA in the right rather than left hemisphere because many studies reported the inhibition function to be right side dominant (Aron, 2007; Aron, Robbins, & Poldrack, 2014). Participants in the sham group underwent the same procedures as the real group, but were treated using a sham coil (Magstim Company).

The personalized target location was computed using TMS target (Ji, Yu, Liao, & Wang, 2017) and SPM12 (www.fil.ion.ucl.ac.uk/spm). First, we defined two regions-of-interest (ROIs), the preSMA and STN. The preSMA was computed from the SMA in Anatomical Automatic Labeling template. The design included SMA voxels anterior to the vertical line passing through anterior commissure (Ji et al., 2017; Johansen-Berg et al., 2004), but excluded SMA voxels from where the shortest distance to the superficial cortex was larger than 15 mm. The STN was a sphere ROI with a center at Montreal Neurological Institute (MNI) coordinates [12, −11, −5], with a radius of 6 mm (Fox et al., 2014; Lozano & Lipsman, 2013). Second, we normalized each individual's T1 image to MNI space and the inverse transformation was applied to the STN and preSMA. Finally, STN-to-preSMA FC was performed in individual space. The preSMA voxel with the highest correlation value was selected as the personalized rTMS target.

2.6 | Baseline and efficacy measures

Demographic information, clinical estimations, and neuropsychological tests were obtained before rTMS treatment. Clinical symptoms were estimated by the Yale–Brown Obsessive Compulsive Scale (YBOCS) before and after treatment. The change of the YBOCS was the primary outcome. We defined responders as patients who showed ≥35% decrease in YBOCS (Pallanti et al., 2002).

2.7 | Statistical analyses

Demographic and clinical symptoms were compared between real and sham groups using the two-sample *t* test (quantitative data) or chi-square test (categorical data). The clinical outcomes were analyzed using two-way (group by time) repeat measure analysis of variance. Post hoc analyses were performed by Bonferroni's multiple comparisons test.

2.8 | Ideal target network

To test our hypothesis that the connectivity pattern of target was related to treatment efficiency, we generated a model of "*ideal target connectivity*" using baseline fMRI data and symptom improvement (percentage change relative to baseline) in two steps (Horn et al., 2017). First, target-to-whole brain FC (Fisher's *z* transformed) was performed for each patient on the preprocessed fMRI data before treatment. Target seed was defined as a sphere centered in the stimulation site with a 6 mm radius. Then, the "*ideal target connectivity*" could be obtained by averaging the connectivity map of the target weighted by YBOCS improvement. Specifically, the percentage symptom changes relative to baseline were individually computed and multiplied by the corresponding target FC map at baseline. Then, the resultant maps were added and averaged by the total symptom changes across patients.

The "*ideal target connectivity*" was tested by leave-one-out cross-validation (LOOCV). First, one patient in the real group was left out as test, while the "*ideal target connectivity*" was computed on the data of the other patients. Second, we computed the spatial correlation coefficient between the connectivity map of test data and "*ideal target connectivity*." Finally, the correlation coefficient (Fisher's *z* transformed) values of patients were correlated to their real improvement in percentage in the YBOCS. A significant correlation ($p < .05$) would support our hypothesis.

2.9 | Target-network mechanism of rTMS

To investigate the role of target network in mediating rTMS aftereffects, positive regions in the "*ideal target connectivity*" map ($p < .0001$) were defined as a seed network (termed "*ideal target network*," [iTN]). The whole-brain FC map of the iTN was constructed using fMRI data before and after treatment. Paired *t* tests were performed between pre- and post-rTMS FC maps at both network and voxel levels.

At the network level, voxels in the comparison map was divided into two networks. One network showed positive correlation with the seed network at baseline, and the other showed negative correlation (both $p < .0001$). The average FC change within each network was compared between groups independently. At the voxel level, the comparison was performed within clusters showing significant correlation with the seed network before treatment ($p < .0001$). The voxel-wise comparison was performed with the SnPM13 toolbox (http://warwick.ac.uk/snpm). Using nonparameter tests, multiple comparisons were corrected at cluster level ($p < .05$) with a cluster-defined threshold of $p < .001$. Notably, the voxel-level comparisons were performed within group-specific masks, but the analyses showed the same cluster threshold, 64 mm^3.

3 | RESULTS

3.1 | Characteristics of patients

Of the 62 patients who completed screening (Figure S1), 44 received treatment. Twenty-three and twenty-one patients were randomly assigned into the real and sham groups, respectively. Seven patients withdrew before the primary end point. Finally, 37 patients (20 real, 17 sham) completed the 14-day treatment. Nine patients did not take any medication 4 weeks before the rTMS treatment. In the other patients, the medication included serotoninergic ($n = 28$), dopaminergic ($n = 14$), and noradrenergic ($n = 4$) drugs, as well as benzodiazepine ($n = 7$). Neither the percentage of medicated patients nor the number of drug types was significantly different between groups (Table 1). Unfortunately, the MRI data of five patients (two real and three sham) were lost during transfer.

Baseline comparison did not show significant differences between groups in demographic, clinical, or neuropsychological tests (Table 1). Based on the baseline MRI data, a personalized target was computed. The target location and connectivity strength to the STN were similar between groups (Table 1, Figure 1a). The average target-to-whole brain FC map showed similar spatial distribution between groups (Dice coefficient = 0.82, Figure 1b). At the end of treatment, all patients were asked, "Are you sure about which group you were assigned?." No positive answer was reported. No severe adverse event was reported during or after the trial in either group.

3.2 | Symptom outcome

There was a significant interaction effect between time (baseline and Week 2) and group (real and sham) in YBOCS ($F_{1,35} = 6.0$, $p = .019$; $\eta^2 = 0.15$; Figure 1c). YBOCS scores (mean ± *SD*) showed a significant decrease in the real group (from 21.0 ± 5.04 at baseline to 14.75 ± 5.33 at Week 2; $p < .0001$; 95% confidence interval [CI], 8.5–4.0; Cohen's $d = 1.21$). A mild but significant decrease was also found in the sham group (from 20.29 ± 5.17 to 17.53 ± 5.76; $p = .02$; 95% CI,

TABLE 1 Baseline measures in real and sham treatment groups

Measures	Real ($n = 20$) Mean ± *SD*	Sham ($n = 17$) Mean ± *SD*	t/X^2	*p*
Demographic data				
Age (years)	27.75 ± 1.58	27.65 ± 1.73	.044[a]	.763
Sex (male/female)	15/5	12/5	—	>.99[b]
Education (years)	14.05 ± 0.50	12.82 ± 0.516	1.700[a]	.098
Illness duration (years)	5.81 ± 0.90	4.24 ± 0.88	1.241[a]	.223
Medication (yes/no)	14/6	14/3	—	.462[b]
No. drug types	1.5 ± 1.40	2.2 ± 1.67	1.34	.19
Symptom estimations				
Y-BOCS total (primary outcome)	21.00 ± 1.13	20.29 ± 1.25	0.420[a]	.677
Y-BOCS obsessive	11.60 ± 0.87	10.94 ± 1.04	0.489[a]	.628
Y-BOCS compulsive	9.40 ± 1.01	9.35 ± 1.23	0.030[a]	.976
HARS	8.05 ± 0.75	6.35 ± 0.73	1.616[a]	.115
HDRS	6.85 ± 0.89	5.94 ± 0.67	0.792[a]	.434
Neuropsychological tests				
TMT A (second)	53.57 ± 4.28	59.69 ± 5.93	0.849[c]	.402
TMT B (second)	98.77 ± 4.46	114.90 ± 11.18	1.393[c]	.173
SCWT (second)	10.93 ± 1.53	8.75 ± 1.35	1.065[d]	.295
DS forward	7.79 ± 0.12	7.88 ± 0.08	0.617[c]	.542
DS backward	5.84 ± 0.23	6.18 ± 0.27	0.935[c]	.356
Target information[c]				
MNI coordinate X	8.33 ± 3.18	9.00 ± 2.35	0.66[d]	.52
MNI coordinate Y	12.33 ± 7.12	9.79 ± 7.08	1.00[d]	.32
MNI coordinate Z	59.50 ± 4.96	62.50 ± 4.49	1.77[d]	.09
zFC to STN	0.11 ± 0.09	0.10 ± 0.08	0.21[d]	.84

Abbreviations: DS, Digit Span; HARS, Hamilton Anxiety Rating Scale; HDRS, Hamilton Depression Rating Scale; MNI, Montreal Neurological Institute; SCWT, Stroop Color Word Test; STN, subthalamic nucleus; TMT, Trail Making Test; Y-BOCS, Yale-Brown Obsessive Compulsive Scale; zFC, Fisher's z transformed functional connectivity.

[a]Paired *t* test.

[b]Fisher's exact test.

[c]One patient in the real group did not compete these tests.

[d]The data were from 18 and 14 patients in the real group and sham group, respectively.

5.21–0.32; Cohen's $d = 0.92$). The percentage change in YBOCS was significantly higher in the real (mean = 29%, $SD = 0.2$) than sham (mean = 14%, $SD = 0.13$) group ($t = 2.9$, $p = .01$; Cohen's $d = 2.50$).

The responder/nonresponder ratio was higher in the real group than in the sham group (chi-square = 4.86, $p = .03$; Figure 1d,e). Specifically, responder criteria (YBOCS reduction ≥35%) were achieved in 9 of 20 patients in the real group, and in 2 of 17 in the sham group. Using a more restrictive criteria of 40%, eight patients were responders in the real group, while no responder was found in the sham group (chi-square = 8.68, $p = .003$).

3.3 | Ideal connectivity pattern of the target

Data from the real group ($n = 18$, Figure 2a) showed that the positive and negative regions in the "*ideal target connectivity*" map ($p < .05$) included regions of the ventral attention network (VAN, e.g., the SMA, anterior insular, supramarginal gyrus [SMG], and posterior cingulate sulcus), and regions of the default mode network (DMN, e.g., inferior parietal lobule, anterior and posterior cingulate cortex [PCC]). Spatially, their Dice coefficients to the VAN and DMN templates (Yeo et al., 2011) were 0.66 and 0.31, respectively.

By using the LOOCV approach, the target connectivity pattern of each patient in the real group was spatially correlated to the "*ideal target connectivity*" map. The correlation coefficient significantly predicted the percentage of symptom improvement after treatment ($r = .60$, $p = .009$; Figure 2b,c). As a control, we performed the same analysis in the sham group. The "*ideal target connectivity*" map of the sham group was different to that of the real group (Figure 2d), and did not predict the symptom improvement in LOOCV ($r = -.004$, $p = 0.99$; Figure 2e).

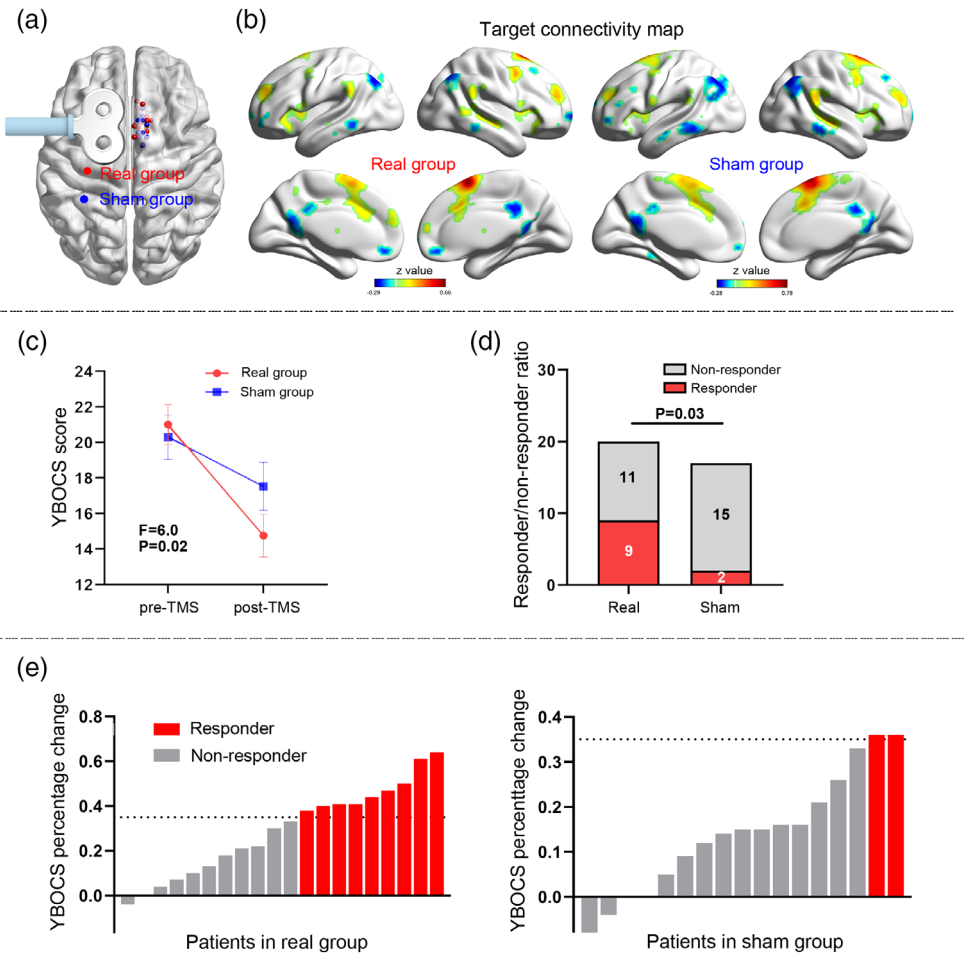

FIGURE 1 Personalized stimulation and outcomes. The targets show similar spatial location (a) and functional connectivity (threshold, $|z| > 0.14$) pattern (b) between groups. The primary outcome (i.e., Yale–Brown Obsessive Compulsive Scale [YBOCS]) decreased more prominently in the real group than in the sham group (c). The responder/nonresponder ratio was higher in the real group than in the sham group (d). YBOCS decreased more than 35% (responder) in nine and two patients from the real group and sham group, respectively (e)

3.4 | Target-network mechanism of rTMS

The connectivity of the iTN to the whole brain was compared between pretreatment and posttreatment data to show functional alterations (Figure 3a,b). The changes were tested at both network and voxel levels. The frame-wise displacement (Power, Barnes, Snyder, Schlaggar, & Petersen, 2012) of head motion was similar between pretreatment and posttreatment conditions for both groups (real group, paired $t = -0.18$, $p = 0.86$; sham group, paired $t = 0.08$, $p = .94$).

At the network level, the whole-brain FC changes were summarized into positive and negative networks, where voxels showed significant synchronization and anticorrelation with the seed network, respectively ($p < .0001$). In the real group, the positive and negative networks showed high spatial overlap with the VAN (Dice coefficient = 0.71) and DMN (Dice coefficient = 0.41), respectively (Figure 3b) (Yeo et al., 2011). Average FC significantly decreased within the positive (paired $t = 5.28$, $p < .001$) and negative (paired $t = 3.11$, $p = .006$; Figure 3c) networks after treatment. In the sham group, the spatial distributions of positive and negative networks were similar to the real group, but no significant longitudinal change was found (paired $t = 1.11$, $p = .29$ for the positive network; paired $t = 1.43$, $p = .18$ for the negative network; Figure 3c).

At the voxel level, the positive network showed deceased connectivity in the left PCC, whereas the negative network showed decreased anticorrelation in the bilateral SMG after treatment (Table S1, Figure 3d). Pearson's correlation analysis indicated that the change (pre- vs. post-rTMS) in the left PCC ($r = .49$, $p = .04$) and right SMG ($r = .56$, $p = .02$) was positively correlated with YBOCS improvement (Figure 3d). No significant FC change was found in the sham group at the voxel level (Figure 3d). In summary, these findings implicated a target-network mechanism whereby the rTMS effect may be achieved by decreasing the FC of the target network.

3.5 | Generalization of target-network mechanism

One schizophrenia and two healthy datasets ($n = 65$) were included to cross-validate the target-network mechanism of rTMS. All data were from previously published works (Chen et al., 2018; Ji et al., 2020). In the schizophrenia cohort, 16 patients received real continuous theta-burst magnetic stimulation (cTBS) over the left temporo-parietal junction. After 2 weeks of treatment, the primary outcome (i.e., auditory hallucination) was significantly alleviated (Chen et al., 2018). In the first healthy cohort, participants were randomly assigned to receive real ($n = 16$) or sham ($n = 17$) cTBS over the left

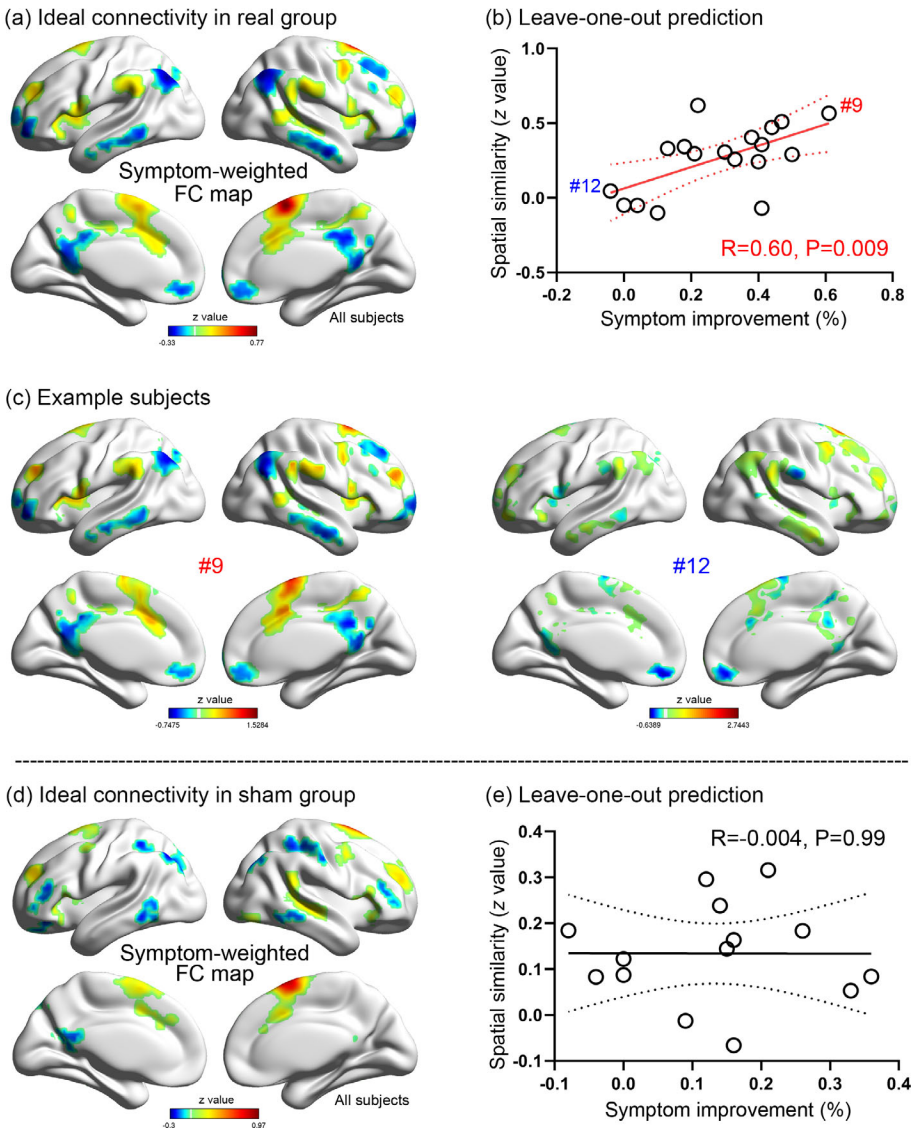

FIGURE 2 Primary outcome prediction. An "*ideal target network*" identified by averaging the symptom-weighted target connectivity map across patients (a). The pattern showing significantly positive connectivity in regions of ventral attention network, such as supramarginal lobule, anterior insular, and cingulate sulcus. Leave-one-out analysis indicating that the Yale–Brown Obsessive Compulsive Scale (YBOCS) improvement predicted by target connectivity map is positively correlated with the real improvement (b). The baseline connectivity pattern of Patients #9 and #12 are shown as examples for responders and nonresponders, respectively (c). An "*ideal target network*" pattern was also computed for the sham group (d), although no predictive value was found (e). Only voxels with absolute *z* value >0.14 are shown in the connectivity maps

SMA for 5 days (Ji et al., 2020). The second healthy cohort ($n = 16$) was recruited to test the reproducibility of the first cohort. The FC change of the target network was analyzed similar to as was done for the OCD data. Briefly, the target network was First defined as regions showing positive FC with the stimulation target at baseline ($p < .0001$). Using the baseline connectivity map of the target network, regions with significant positive or negative FC could be identified ($p < .0001$). Then, the absolute change of these regions were averaged and compared between pre- and post-rTMS conditions by using paired *t* tests.

The schizophrenia group received 2-weeks cTBS treatment ($n = 16$), and showed decreased FC of the target network ($t = 3.54$, $p = .003$; Figure 4a). The percentage improvement of auditory verbal hallucination (pre- minus post-data, divided by pre-data) was positively correlated to the decreased FC of the target network ($r = .64$, $p = .008$; Figure 5). Similarly, decreased FC was found in the real group of the first healthy cohort ($n = 16$, $t = 4.36$, $p = .0006$; Figure 4b), while the change in the sham group was not significant ($n = 17$, $t = 0.66$, $p = 0.52$). The second healthy group had a similar FC change ($n = 16$, $t = 2.52$, $p = .02$; Figure 4b) as the first. These findings suggested that the target-network mechanism of rTMS could be generalized to other protocols regardless of the target location and stimulation sequence.

Supplementary analysis

We performed two batteries of analyses to show the specificity and robustness of our main findings.

1. We repeated the LOOCV of the real group using two additional conditions
   a. To test whether the LOOCV was exclusively caused by the symptom improvement variance across patients, we intentionally mismatched the symptom changes and patients.
   b. To test whether the LOOCV was specific to the right preSMA, we flipped all targets to the left hemisphere. Under both conditions, LOOCV did not show significant correlation between the predictive and actual symptom improvement (Figure S2).

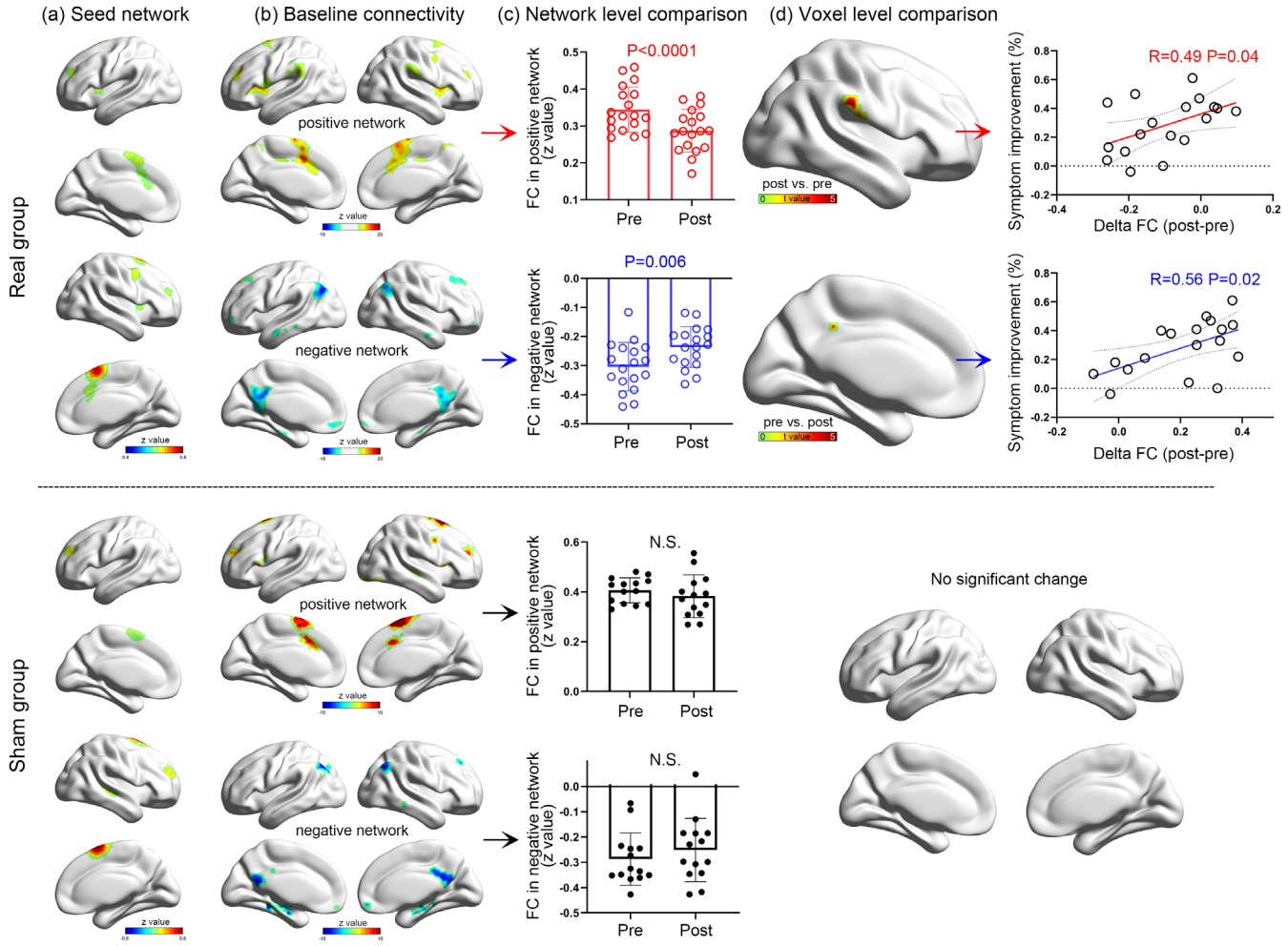

FIGURE 3 Connectivity change of the ideal target network. The ideal target network showing different spatial patterns between groups (a). We took voxels positively or negatively correlating with the seed network at baseline (b) as two regions-of-interest. Their connectivity strength to the seed network significantly decreased in the real group but not in the sham group (c). Voxel-wise comparison between pretreatment and posttreatment conditions showing significant connectivity strength decreases in the posterior cingulate cortex and supramarginal gyrus in the real group (d). No significant region was found in the sham group. Positive imaging-symptom correlation showing a more prominent connectivity change predicting better symptom improvement (D)

2. To show network mechanism, we defined a seed network in the ITN and showed its connectivity change after treatment
   a. The iTN was initially defined by a harsh threshold ($p < .0001$), since strong connections were more likely to engage in the aftereffect propagation than weak connections. Here, we reported that the FC decrease of the target network could be replicated in weak thresholds, 0.001 and 0.01. Under both conditions, the positive and negative networks showed significant FC changes after real treatment, but not after sham treatment (Figure S3).
   b. To maximally identify the FC change after treatment, we defined the iTN (i.e., seed network) of each group independently. Statistically, the FC change of different seeds was not comparable. Thus, the change in the real group may be mainly caused by placebo effect. Here, we re-estimated the FC change in the sham group using the seed network in the real group, which made the FC change between groups comparable. Then, two-way repeated-measure analysis of variance was performed for the average FC in the positive and negative networks independently (Figure S4). Significant interaction effect (group by time) was found for the positive network ($F = 5.82$, $p = .02$). Simple-effect analysis showed significant FC decrease in the real group ($t = 5.28$, $p < .001$), but not in the sham group ($t = 0.19$, $p = .98$). However, the interaction effect was not significant for the negative network ($F = 1.51$, $p = .23$).

4 | DISCUSSION

This study investigated the neural mechanism of rTMS on OCD patents in the context of a randomized clinical trial. There were four main findings. First, the alleviation of obsessive–compulsive symptoms was greater in the real group than in the sham group. Importantly, 45% of patients in the real group were responsive to the treatment. Second,

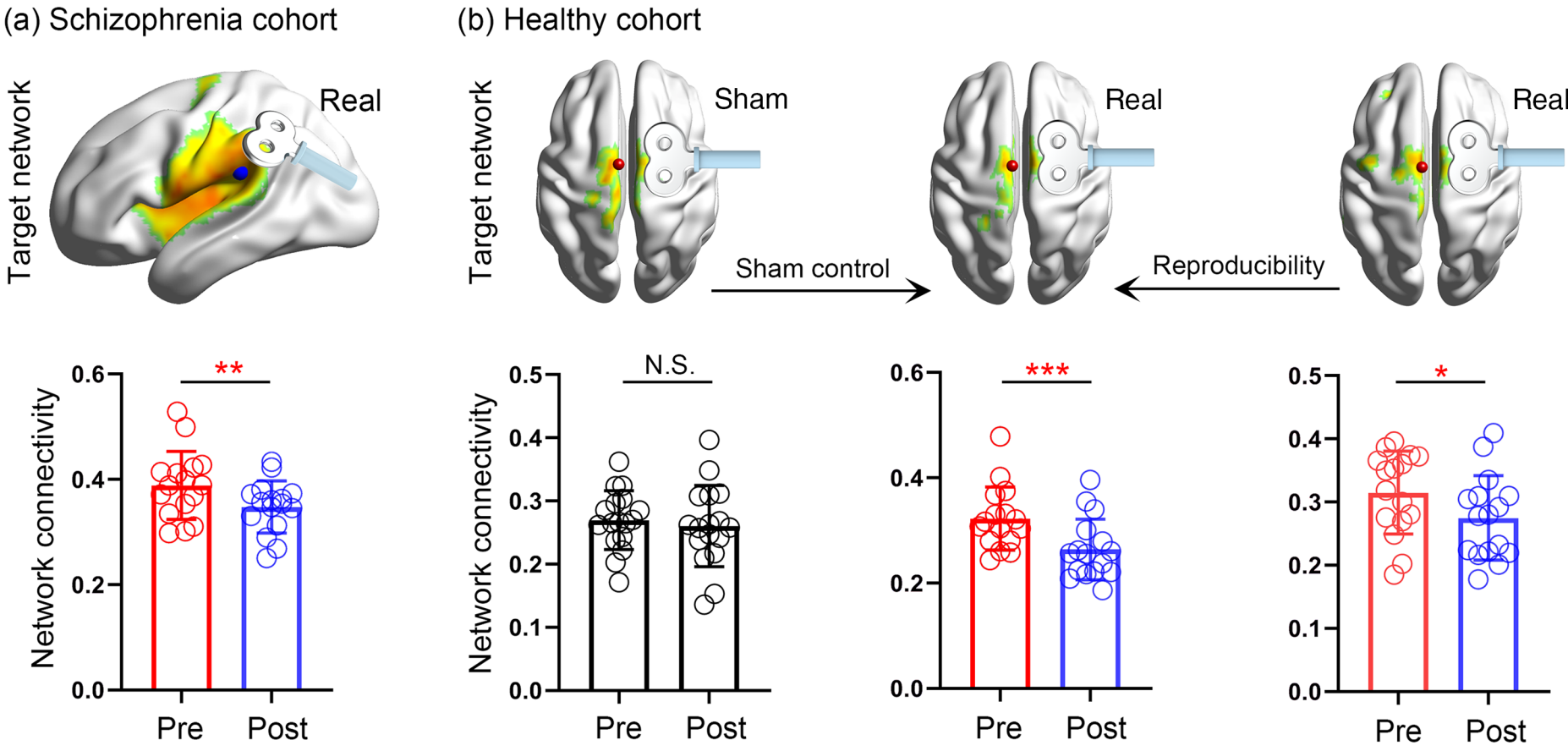

FIGURE 4 Cross-validation of the target network mechanism. This independent validation was performed on schizophrenia (a) and healthy participants (b). The schizophrenia patients received real continuous theta-burst magnetic stimulation (cTBS) treatment over the temporo-parietal junction for 2 weeks and showed significant symptom alleviation. Two groups of healthy participants were randomly assigned to receive real or sham cTBS over the supplementary motor area for 5 days. The second real group was used to test the reproducibility of the findings. The target network was defined as the regions showing significant functional connectivity with the target area ($p < .0001$). The absolute connectivity strength of the target network significantly decreased in all of the real groups, and no change was found in the sham group. $^{*}p < .05$, $^{**}p < .01$, $^{***}p < .001$

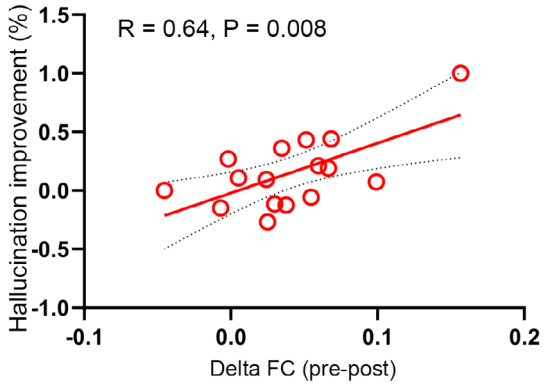

FIGURE 5 Correlation between connectivity and symptom changes in the schizophrenia cohort. The connectivity change of target (i.e., temporo-parietal cortex) network was positively correlated with auditory verbal hallucination improvement after treatment

the spatial similarity of each patient's target network to the ideal connectivity pattern was predictive of symptom improvement. Third, the whole-brain connectivity strength of the iTN was significantly deceased after real treatment. The greater was the FC changes in the PCC and SMG, the better the YBOCS improvement. Finally, this network mechanism of rTMS was further validated in three independent datasets, suggesting its generalizability to other long-term rTMS protocols.

The potential of rTMS in alleviating OCD symptoms has been investigated by many randomized clinical trials (Carmi et al., 2018; Harika-Germaneau et al., 2019; Rehn et al., 2018). However, the findings in clinical efficacy were inconsistent, which may be related to differences in the rTMS setting. A meta-analysis showed that low-frequency rTMS applied over the SMA may offer the greatest effectiveness in alleviating symptoms associated with OCD (Rehn et al., 2018). Consistent with this prediction, we found that 1-Hz rTMS over the preSMA significantly decreased the symptoms of OCD patients. Particularly, the personalized target defined by the STN connectivity map may have positively contributed to the symptom improvement (Cocchi & Zalesky, 2018; Fox et al., 2014). With the current optimized protocol, 45% patients were responsive to the real treatment. This ratio was comparable to a current deep rTMS study on OCD (38.1%) (Carmi et al., 2019). Interestingly, the sham group showed a mild but significant symptom improvement in our study. A similar phenomenon was also found in previous studies on OCD (Harika-Germaneau et al., 2019), depression (Li et al., 2020) and schizophrenia (Dollfus, Lecardeur, Morello, & Etard, 2016). These findings indicate a considerable placebo effect in patients with psychiatry disorders, and emphasize the importance of sham controls in rTMS studies. Additionally, the relatively lax control in medication may also contribute to this symptom improvement after sham rTMS. We required that the drug dose should be fixed 4 weeks before rTMS treatment. However, patients may have benefited from longer medication therapy. To exclude the potential effect of medication, future studies should prolong the observation period to 12 weeks.

Although both TMS and DBS are techniques used to stimulate local brain areas, the effects may influence regions anatomically remote to the initial target. It has been suggested that the functional or structural connectivity of the target plays a crucial role in the propagation of the aftereffects (Castrillon et al., 2020; Fox et al., 2014; Lynch et al., 2019; Sale, Mattingley, Zalesky, & Cocchi, 2015). In Parkinson's disease, the connectivity pattern of the DBS target showed high predictive value in the clinical outcome (Horn et al., 2017). By a similar approach, we identified an ideal connectivity pattern using baseline connectivity map and symptom improvement. In the real group, the ideal target connectivity included positive and negative regions in the VAN and DMN, respectively (Yeo et al., 2011). These findings suggested that the optimal preSMA target may be a node of the VAN. LOOCV indicated that the individual outcome could be predicted by the spatial similarity between the individual's target network and the ideal pattern. The spatial difference of the target network explained 36% of the variance in symptom alleviation. The baseline connectivity based prediction may help clinicians to more prudently allocate resources for this time-consuming treatment.

To show functional changes mediated by the target network, we chose the iTN as a seed network. At the network level, significant alterations were found in the positive network, as well as the negative (or anticorrelated) network after real treatment. Interestingly, only decreased connectivity strength was found, implicating that the treatment inhibited or isolated the function of the target network. The positive and negative networks showed high spatial overlap with the VAN and DMN, respectively (Yeo et al., 2011), where the functional reorganization may be related to symptom alleviation. These results were supported by our imaging-behavior correlation findings. The engagement of attention network was in line with a deep TMS study that found electroencephalogram changes in attention tasks were associated with symptom improvement in OCD (Carmi et al., 2018). In the negative network, the anticorrelation in the PCC was significantly decreased with YBOCS improvement. The PCC, a hub region of the DMN, was found to be associated with self-referential processing (Maki-Marttunen, Castro, Olmos, Leiguarda, & Villarreal, 2016; Sheline et al., 2009). Functional abnormality of the DMN partly contributed to self-oriented repetitive obsessions in OCD patients (Reggente et al., 2018). Our findings in the PCC implicated a dissociation between the DMN and VAN after treatment. This change may release the patients' attention from self-reference processing to externally oriented cognition, and finally decrease the obsessive–compulsive symptoms.

Some limitations of this study should be mentioned. First, this was a single-center study with a small sample size. Besides the network mechanism, which was validated using three independent datasets, the clinical efficacy of the treatment protocol needs to be further validated using a multisite dataset. Second, although the iTN showed significantly predictive value for symptom outcome, an independent dataset is still necessary to demonstrate its generalization in clinical application. Third, this study aimed to investigate the mechanism of rTMS treatment on OCD, rather than to compare clinical efficacy between FC-based and traditional rTMS protocol. Thus, we did

not include a control group that received real rTMS without FC-based target definition, and our clinical findings cannot demonstrate whether the FC-based rTMS is better than traditional rTMS in clinical efficacy. Fourth, all the rTMS protocols in the validation analysis were inhibitory sequences that could decrease the excitability of the target. Whether the mechanism can be generalized to an excitatory sequence (i.e., 10 or 20 Hz) needs further investigation. Finally, OCD patients with comorbidities were excluded from this study because we aimed to explore the rTMS effect in OCD symptoms rather than other psychiatric symptoms or their interactions. This is also an effective approach to exclude confounding factors in small sample studies. Future studies are necessary to determine whether our findings can be generalized to OCD patients with comorbidities.

5 | CONCLUSIONS

In this study, we found that the active rTMS treatment significantly alleviated the clinical symptoms of OCD. The outcome variability across patients could be largely explained by the baseline connectivity pattern of the stimulation target. Symptom improvement was significantly correlated with the connectivity change between the target network and VAN/DMN regions. Together, our findings suggested that the rTMS on pre-SMA may effectively alleviate obsessive–compulsive symptoms by decreasing the whole-brain connectivity strength of the target network.

ACKNOWLEDGMENTS

The authors would like to thank Information Science Laboratory Center of USTC for the measurement services, and all the participants. This study was funded by the National Natural Science Foundation of China, Grant Numbers: 81771456, 31970979, 81971689, 8180111185, 82001429, 31771222, and 31571149; the Doctoral Foundation of Anhui Medical University, Grant Number: XJ201532; the National Basic Research Program of China, Grant Number: 2015CB856405; the National Key R&D Plan of China, Grant Number: 2016YFC1300604; the Collaborative Innovation Center of Neuropsychiatric Disorders and Mental Health of Anhui Province; and the Youth Top-notch Talent Support Program of Anhui Medical University.

CONFLICT OF INTERESTS

The authors declare no conflict of interest.

DATA AVAILABILITY STATEMENT

The data that support the findings of this study are available on request from the corresponding author.

ORCID

Gong-Jun Ji https://orcid.org/0000-0002-7073-5534
Tongjian Bai https://orcid.org/0000-0002-2185-0042
Kai Wang https://orcid.org/0000-0002-6197-914X

REFERENCES

Aron, A. R. (2007). The neural basis of inhibition in cognitive control. *The Neuroscientist*, *13*, 214–228.

Aron, A. R., Robbins, T. W., & Poldrack, R. A. (2014). Inhibition and the right inferior frontal cortex: One decade on. *Trends in Cognitive Sciences*, *18*, 177–185.

Bari, A., & Robbins, T. W. (2013). Inhibition and impulsivity: Behavioral and neural basis of response control. *Progress in Neurobiology*, *108*, 44–79.

Beynel, L., Powers, J. P., & Appelbaum, L. G. (2020). Effects of repetitive transcranial magnetic stimulation on resting-state connectivity: A systematic review. *NeuroImage*, *211*, 116596.

Carmi, L., Alyagon, U., Barnea-Ygael, N., Zohar, J., Dar, R., & Zangen, A. (2018). Clinical and electrophysiological outcomes of deep TMS over the medial prefrontal and anterior cingulate cortices in OCD patients. *Brain Stimulation*, *11*, 158–165.

Carmi, L., Tendler, A., Bystritsky, A., Hollander, E., Blumberger, D. M., Daskalakis, J., … Zohar, J. (2019). Efficacy and safety of deep transcranial magnetic stimulation for obsessive-compulsive disorder: A prospective multicenter randomized double-blind placebo-controlled trial. *The American Journal of Psychiatry*, *176*, 931–938.

Castrillon, G., Sollmann, N., Kurcyus, K., Razi, A., Krieg, S. M., & Riedl, V. (2020). The physiological effects of noninvasive brain stimulation fundamentally differ across the human cortex. *Science Advances*, *6*, eaay2739.

Chen, X., Ji, G. J., Zhu, C., Bai, X., Wang, L., He, K., … Wang, K. (2018). Neural correlates of auditory verbal hallucinations in schizophrenia and the therapeutic response to theta-burst transcranial magnetic stimulation. *Schizophrenia Bulletin*, *45*(2), 474–483.

Cocchi, L., & Zalesky, A. (2018). Personalized transcranial magnetic stimulation in psychiatry. *Biological Psychiatry. Cognitive Neuroscience and Neuroimaging*, *3*, 731–741.

Dollfus, S., Lecardeur, L., Morello, R., & Etard, O. (2016). Placebo response in repetitive transcranial magnetic stimulation trials of treatment of auditory hallucinations in schizophrenia: A meta-analysis. *Schizophrenia Bulletin*, *42*, 301–308.

Fox, M. D., Buckner, R. L., Liu, H., Chakravarty, M. M., Lozano, A. M., & Pascual-Leone, A. (2014). Resting-state networks link invasive and noninvasive brain stimulation across diverse psychiatric and neurological diseases. *Proceedings of the National Academy of Sciences of the United States of America*, *111*, E4367–E4375.

Fox, M. D., Buckner, R. L., White, M. P., Greicius, M. D., & Pascual-Leone, A. (2012). Efficacy of transcranial magnetic stimulation targets for depression is related to intrinsic functional connectivity with the subgenual cingulate. *Biological Psychiatry*, *72*, 595–603.

Fox, P. T., Narayana, S., Tandon, N., Sandoval, H., Fox, S. P., Kochunov, P., & Lancaster, J. L. (2004). Column-based model of electric field excitation of cerebral cortex. *Human Brain Mapping*, *22*, 1–14.

Friston, K. J., Williams, S., Howard, R., Frackowiak, R. S., & Turner, R. (1996). Movement-related effects in fMRI time-series. *Magnetic Resonance in Medicine*, *35*, 346–355.

Hampshire, A., & Sharp, D. J. (2015). Contrasting network and modular perspectives on inhibitory control. *Trends in Cognitive Sciences*, *19*, 445–452.

Harika-Germaneau, G., Rachid, F., Chatard, A., Lafay-Chebassier, C., Solinas, M., Thirioux, B., … Jaafari, N. (2019). Continuous theta burst stimulation over the supplementary motor area in refractory obsessive-compulsive disorder treatment: A randomized sham-controlled trial. *Brain Stimulation*, *12*, 1565–1571.

Hawken, E. R., Dilkov, D., Kaludiev, E., Simek, S., Zhang, F., & Milev, R. (2016). Transcranial magnetic stimulation of the supplementary motor area in the treatment of obsessive-compulsive disorder: A multi-site study. *International Journal of Molecular Sciences*, *17*, 420.

Heyman, I., Mataix-Cols, D., & Fineberg, N. A. (2006). Obsessive-compulsive disorder. *BMJ*, *333*, 424–429.

Horn, A., Reich, M., Vorwerk, J., Li, N., Wenzel, G., Fang, Q., … Fox, M. D. (2017). Connectivity predicts deep brain stimulation outcome in Parkinson disease. *Annals of Neurology*, *82*, 67–78.

Janssen, A. M., Oostendorp, T. F., & Stegeman, D. F. (2015). The coil orientation dependency of the electric field induced by TMS for M1 and other brain areas. *Journal of Neuroengineering and Rehabilitation*, *12*, 47.

Ji, G. J., Ren, C., Li, Y., Sun, J., Liu, T., Gao, Y., … Wang, K. (2018). Regional and network properties of white matter function in Parkinson's disease. *Human Brain Mapping*, *40*(4), 1253–1263.

Ji, G. J., Sun, J., Liu, P., Wei, J., Li, D., Wu, X., … Wang, K. (2020). Predicting long-term after-effects of theta-burst stimulation on supplementary motor network through one-session response. *Frontiers in Neuroscience*, *14*, 237.

Ji, G. J., Yu, F., Liao, W., & Wang, K. (2017). Dynamic aftereffects in supplementary motor network following inhibitory transcranial magnetic stimulation protocols. *NeuroImage*, *149*, 285–294.

Johansen-Berg, H., Behrens, T. E., Robson, M. D., Drobnjak, I., Rushworth, M. F., Brady, J. M., … Matthews, P. M. (2004). Changes in connectivity profiles define functionally distinct regions in human medial frontal cortex. *Proceedings of the National Academy of Sciences of the United States of America*, *101*, 13335–13340.

Koran, L. M., Hanna, G. L., Hollander, E., Nestadt, G., & Simpson, H. B. (2007). Practice guideline for the treatment of patients with obsessive–compulsive disorder. *The American Journal of Psychiatry*, *164*(7 Suppl), 5e53.

Lefaucheur, J. P., Aleman, A., Baeken, C., Benninger, D. H., Brunelin, J., Di Lazzaro, V., … Ziemann, U. (2020). Evidence-based guidelines on the therapeutic use of repetitive transcranial magnetic stimulation (rTMS): An update (2014-2018). *Clinical Neurophysiology*, *131*, 474–528.

Li, C. T., Cheng, C. M., Chen, M. H., Juan, C. H., Tu, P. C., Bai, Y. M., … Su, T. P. (2020). Antidepressant efficacy of prolonged intermittent theta burst stimulation monotherapy for recurrent depression and comparison of methods for coil positioning: A randomized, double-blind, sham-controlled study. *Biological Psychiatry*, *87*, 443–450.

Lozano, A. M., & Lipsman, N. (2013). Probing and regulating dysfunctional circuits using deep brain stimulation. *Neuron*, *77*, 406–424.

Lynch, C. J., Breeden, A. L., Gordon, E. M., Cherry, J. B. C., Turkeltaub, P. E., & Vaidya, C. J. (2019). Precision inhibitory stimulation of individual-specific cortical hubs disrupts information processing in humans. *Cerebral Cortex*, *29*, 3912–3921.

Maki-Marttunen, V., Castro, M., Olmos, L., Leiguarda, R., & Villarreal, M. (2016). Modulation of the default-mode network and the attentional network by self-referential processes in patients with disorder of consciousness. *Neuropsychologia*, *82*, 149–160.

Mallet, L., Polosan, M., Jaafari, N., Baup, N., Welter, M. L., Fontaine, D., … Pelissolo, A. (2008). Subthalamic nucleus stimulation in severe obsessive-compulsive disorder. *The New England Journal of Medicine*, *359*, 2121–2134.

Pallanti, S., Hollander, E., Bienstock, C., Koran, L., Leckman, J., Marazziti, D., … Zohar, J. (2002). Treatment non-response in OCD: Methodological issues and operational definitions. *The International Journal of Neuropsychopharmacology*, *5*, 181–191.

Power, J. D., Barnes, K. A., Snyder, A. Z., Schlaggar, B. L., & Petersen, S. E. (2012). Spurious but systematic correlations in functional connectivity MRI networks arise from subject motion. *NeuroImage*, *59*, 2142–2154.

Reggente, N., Moody, T. D., Morfini, F., Sheen, C., Rissman, J., O'Neill, J., & Feusner, J. D. (2018). Multivariate resting-state functional connectivity predicts response to cognitive behavioral therapy in obsessive-compulsive disorder. *Proceedings of the National Academy of Sciences of the United States of America*, *115*, 2222–2227.

Rehn, S., Eslick, G. D., & Brakoulias, V. (2018). A meta-analysis of the effectiveness of different cortical targets used in repetitive transcranial magnetic stimulation (rTMS) for the treatment of obsessive-compulsive disorder (OCD). *The Psychiatric Quarterly*, *89*, 645–665.

Ruscio, A. M., Stein, D. J., Chiu, W. T., & Kessler, R. C. (2010). The epidemiology of obsessive-compulsive disorder in the National Comorbidity Survey Replication. *Molecular Psychiatry*, *15*, 53–63.

Sale, M. V., Mattingley, J. B., Zalesky, A., & Cocchi, L. (2015). Imaging human brain networks to improve the clinical efficacy of non-invasive brain stimulation. *Neuroscience and Biobehavioral Reviews*, *57*, 187–198.

Shafiei, G., Markello, R. D., Makowski, C., Talpalaru, A., Kirschner, M., Devenyi, G. A., … Misic, B. (2020). Spatial patterning of tissue volume loss in schizophrenia reflects brain network architecture. *Biological Psychiatry*, *87*, 727–735.

Sheline, Y. I., Barch, D. M., Price, J. L., Rundle, M. M., Vaishnavi, S. N., Snyder, A. Z., … Raichle, M. E. (2009). The default mode network and self-referential processes in depression. *Proceedings of the National Academy of Sciences of the United States of America*, *106*, 1942–1947.

Soomro, G. M., Altman, D., Rajagopal, S., & Oakley-Browne, M. (2008). Selective serotonin re-uptake inhibitors (SSRIs) versus placebo for obsessive compulsive disorder (OCD). *Systematic Reviews*, *1*, CD001765.

Van Ameringen, M., Patterson, B., & Simpson, W. (2014). DSM-5 obsessive-compulsive and related disorders: Clinical implications of new criteria. *Depression and Anxiety*, *31*, 487–493.

Weigand, A., Horn, A., Caballero, R., Cooke, D., Stern, A. P., Taylor, S. F., … Fox, M. D. (2017). Prospective validation that subgenual connectivity predicts antidepressant efficacy of transcranial magnetic stimulation sites. *Biological Psychiatry*, *84*(1), 28–37.

Yau, Y., Zeighami, Y., Baker, T. E., Larcher, K., Vainik, U., Dadar, M., … Dagher, A. (2018). Network connectivity determines cortical thinning in early Parkinson's disease progression. *Nature Communications*, *9*, 12.

Yeo, B. T., Krienen, F. M., Sepulcre, J., Sabuncu, M. R., Lashkari, D., Hollinshead, M., … Buckner, R. L. (2011). The organization of the human cerebral cortex estimated by intrinsic functional connectivity. *Journal of Neurophysiology*, *106*, 1125–1165.

Zhou, J., Gennatas, E. D., Kramer, J. H., Miller, B. L., & Seeley, W. W. (2012). Predicting regional neurodegeneration from the healthy brain functional connectome. *Neuron*, *73*, 1216–1227.

SUPPORTING INFORMATION

Additional supporting information may be found online in the Supporting Information section at the end of this article.

How to cite this article: Ji, G.-J., Xie, W., Yang, T., Wu, Q., Sui, P., Bai, T., Chen, L., Chen, L., Chen, X., Dong, Y., Wang, A., Li, D., Yang, J., Qiu, B., Yu, F., Zhang, L., Luo, Y., Wang, K., & Zhu, C. (2021). Pre-supplementary motor network connectivity and clinical outcome of magnetic stimulation in obsessive–compulsive disorder. *Human Brain Mapping*, *42*(12), 3833–3844. https://doi.org/10.1002/hbm.25468